ANNALI DI GEOFISICA, VOL. XXXVIII, N. 2, May 1995

Main shock and aftershocks of the December 13, 1990, Eastern Sicily earthquake

Alessandro Amato, Riccardo Azzara, Alberto Basili, Claudio Chiarabba, Massimo Cocco, Massimo Di Bona and Giulio Selvaggi
Istituto Nazionale di Geofisica, Roma, Italy

Abstract
In this paper we describe the location and the fault plane solution of the December 13, 1990, Eastern Sicily earthquake ($M_L = 5.4$), and of its aftershock sequence. Because the main shock location is not well constrained due to the geometry of the permanent National Seismic Network in this area, we used a «master event» algorithm to locate it in relation to a well located aftershock. The revised location is slightly offshore Eastern Sicily, 4.8 km north of the largest aftershock ($M_L = 4.6$) that occurred on December 16, 1990. The main shock has a strike-slip mechanism, indicating SE-NW compression with either left lateral motion on a NS plane, or right lateral on an EW plane. Two days after the main event we deployed a local network of eight digital stations, that provided accurate locations of the aftershocks, and the estimate of source parameters for the strongest earthquake. We observed an unusual quiescence after the $M_L = 5.4$ event, that lasted until December 16, when a $M_L = 4.6$ earthquake occurred. The fault plane solution of this aftershock shows normal faulting on E-W trending planes. Between December 16 and January 6, 1991, a sequence of at least 300 aftershocks was recorded by the local network. The well located earthquakes define a small source region of approximately $5 \times 2 \times 5$ km^3, with hypocentral depths ranging between 15 and 20 km. The paucity of large aftershocks, the time gap between the main shock occurrence and the beginning of the aftershock sequence (3.5 days), their different focal mechanisms (strike-slip vs. normal), and the different stress drop between main shock and aftershock suggest that the $M_L = 5.4$ earthquake is an isolated event. The sequence of aftershocks began with the $M_L = 4.6$ event, which is probably linked to the main shock with a complex mechanism of stress redistribution after the main faulting episode.

Key words *seismicity – focal mechanism – local networks – Eastern Sicily earthquake*

1. Introduction

On December 13, 1990, at 00:24 UTC (01:24 in Italy), many towns of Eastern Sicily were woken up by a $M_L = 5.4$ earthquake, that produced extensive damage in a broad region and 19 casualities. The first fully automatic location of the Istituto Nazionale di Geofisica was offshore the Gulf of Noto (36.90N, 15.68E). A subsequent revised location moved the hypocenter to offshore Augusta (37.33N, 15.28E, see fig. 1). The earthquake occurred in a complex tectonic setting, *i.e.*, the junction between the Apenninic-Meghrebide chain and the African foreland, about 40 km to the south of the active basaltic volcano of Mt. Etna. From south to north three main structural units have been recognized, namely the Iblean foreland, the Gela-Catania foredeep (see fig. 1), and the Northern Sicilian compressional margin (Carbone *et al.*, 1982). Offshore Syracuse, the Ibleo-Maltese scarp bounds the system of NE-SW trending thrusts and folds on the Ionian (eastern) side (fig. 1). The Ibleo-Maltese scarp connects the Sicilian foreland and foredeep

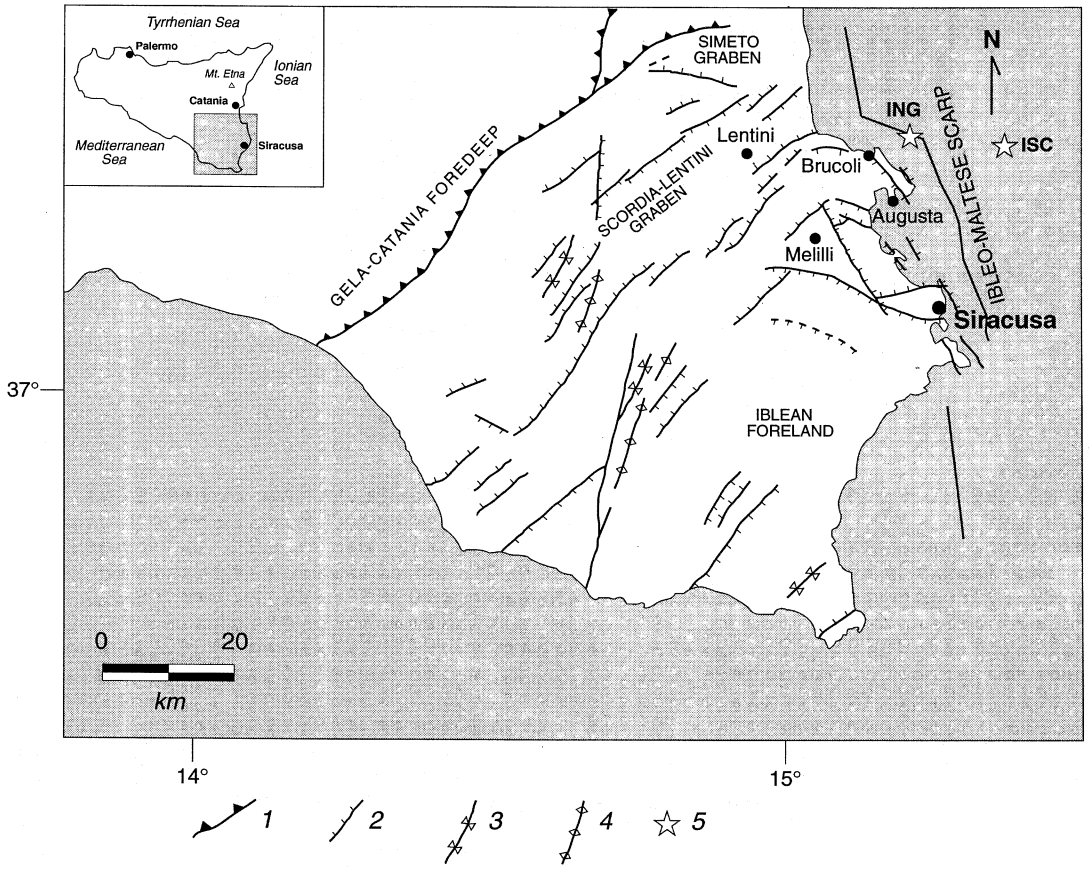

Fig. 1. Geologic map of Southeastern Sicily. The main tectonic structures have been drawn: 1) main thrust faults; 2) normal faults; 3) syncline axes; 4) anticline axes; 5) mainshock epicenters from ING (ING-3) and ISC (modified after Bianchi *et al.*, 1987).

with the oceanic crust of the Ionian sea, with a morphological step of more than 1 km in a distance range of about 10 km.

In the last 1000 years, this area was struck by large seismic events (1169, XI MCS; 1542, IX MCS; and 1693, XI MCS, Mercalli-Cancani-Sieberg macroseismic scale; see P.F.G., 1985), and is one of the regions with the highest seismic hazard in Italy (Barbano and Cosentino, 1981). The 1693 event is the best documented destructive earthquake in this area that produced huge damage in a wide region (P.F.G., 1985; Boschi *et al.*, 1994). Using an empirical relationship between seismic moment and the area of isoseismal curves from many Italian earthquakes, we have a rough estimate of the scalar moment for this earthquake of about $\approx 10^{27}$ dyne·cm, (A. Rovelli written communication, 1994). This value can be considered representative of the seismogenic potential in this region, and it implies that the expected magnitude for a characteristic earthquake occurring in this area is larger than $M \sim 7$.

The remarkable potential for large earthquakes in this region spurred us to investigate

in detail the December 1990 seismic sequence. Therefore, within two days from the $M_L = 5.4$ earthquake, we installed a digital telemetered mobile network in the area, that allowed real-time monitoring of the aftershock activity. In about 20 days of operation, the network recorded more than 300 earthquakes, providing original information for the area. The seismic activity ceased within one month from the main shock. Subsequently, we improved the detection level of the permanent National Network by installing a new three component station close to the epicentral area of the 1990 seismic sequence, near the town of Augusta.

In this paper we discuss the hypocentral locations, the focal mechanisms and the earthquake size of the main shock and of the aftershocks.

2. The main shock of December 13, 1990

The December 13, $M_L = 5.4$, earthquake was preceded by two small earthquakes which occurred on December 3. Then, after eight days of quiescence, three more seismic events were recorded in the same area during December 11 and 12. Due to their small magnitude (ranging between 2.1 and 2.4) we cannot compute reliable hypocentral locations of these «foreshocks». We attribute these events to the same region of the main shock, based on the *S-P* arrival times observed at the closest available stations.

On December 13, 1990 at 00.24 UTC the $M_L = 5.4$ main shock occurred. The magnitude was estimated by the VBB (Very Broad Band) station VSL, belonging to the MEDNET seismic network (S. Mazza written communication, 1991). The seismic moment, estimated by inverting broad-band waveforms at regional distances, is $M_0 = 3.7 \times 10^{24}$ dyne·cm, that corresponds to a moment magnitude of $M_W = 5.7$ (Giardini *et al.*, 1994). According to ISC bulletins, m_b ranges between 5.1 and 5.7, M_S between 5.0 and 5.3, and the scalar moment is 3.3×10^{24} dyne·cm.

The main shock was first located offshore Southeastern Sicily (36.90N, 15.68E) by the automatic earthquake location algorithm (Basili *et al.*, 1990) routinely used at the Istituto Nazionale di Geofisica, ING, (location ING-1 in table I). Then the main shock location was revised including the arrival times at seismic stations of local networks. The revised epicenter is at 37.34N, 15.26E (ING-2 in table I), very close to the aftershock locations, as will be shown in a later section. Table I reports the different locations and magnitudes reported by many agencies.

We have also relocated the main shock relative to the $M_L = 4.6$ event of December 16, selected as the «master» event, because its hypocentral errors are in the order of 1 km (information on the velocity model will be reported in a later section). To perform the relative location, we used the arrival times at the seismic stations of the National Seismic Network that recorded both the earthquakes. The results show that the main shock epicenter is located N14°E and 4.8 km away from the master event (location ING-3 in table I) with hori-

Table I. Hypocentral parameters of the main shock.

Agencies	Latitude	Longitude	Depth	*M*
ING-1 (automatic)	36.90 ± 10	15.68 ± 6	10 (fixed)	4.7 (*Md*)
ING-2 (revised)	37.34 ± 2	15.26 ± 3	18 ± 5	5.4 (*Ml*)
ING-3 (master)	37.32 ± 1	15.25 ± 1	22 ± 2	5.4 (*Ml*)
NEIC	37.30	15.44	11 (*pP-P*)	5.5 (*Mb*)
ISC	37.31	15.43	10 (fixed)	5.3 (*Mb*)
HDRV (CMT)	37.25	14.90	15	5.7 (*Mw*)

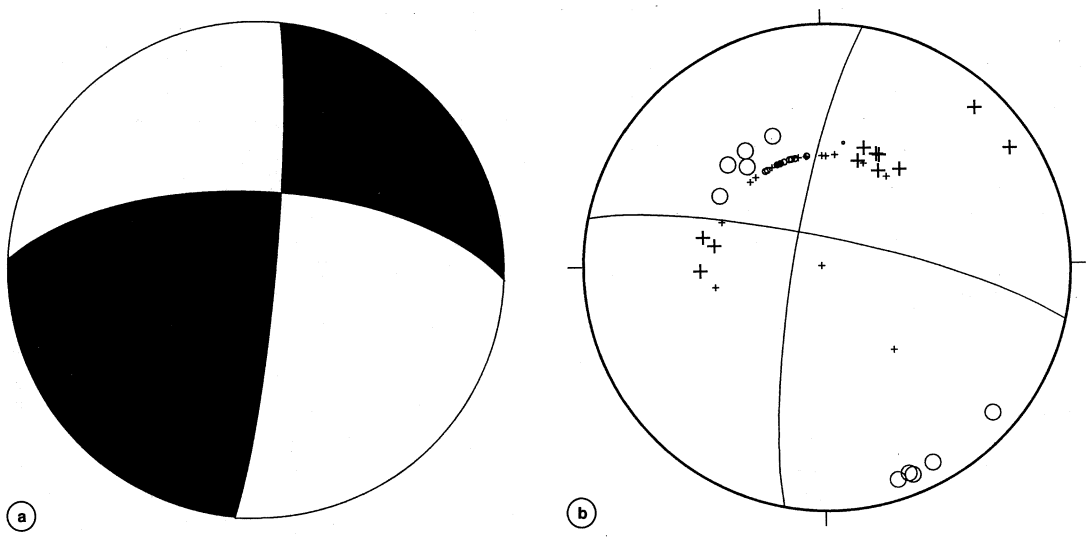

Fig. 2a,b. Fault plane solutions of the main shock: a) CMT solution (Giardini *et al.*, 1994); b) only checked polarities from ING stations (*Pn* polarities have a smaller weight).

zontal errors of 1 km. Table I summarizes the results of the relative location and shows the hypocentral locations computed by different institutions. This location (ING-3) is only within 2-3 km from the revised location reported as ING-2 in table I. We still have uncertainties on the main shock hypocentral depth. The relative location yields an estimate of 22 ± 2 km, whereas *pP-P* observations reported by the ISC give a shallower value of 11 ($\pm$ 2) km.

Different fault plane solutions are available for the 1990 Eastern Sicily earthquake. We compare the CMT solution and that resulting from the moment tensor inversion (Giardini *et al.*, 1994), with the focal mechanism computed in this study from *P*-wave polarities. The comparison is made by reporting strike, dip, and rake of one of the two conjugate planes; here we report these values for the NS plane. The CMT fault plane solution shows an almost pure strike-slip mechanism, with either left-lateral motion on a N-S vertical plane, or right-lateral motion on an E-W, 62° N-dipping plane. The CMT solution is shown in fig. 2a: the NS plane strikes N06°E, dipping 84° East, with a rake angle of 26°. The focal mechanism resulting from the moment tensor inversion, computed by Giardini *et al.* (1994) by modeling the long period waveforms recorded at regional distances, shows a NS plane striking N04°E, dipping 82° East and with a rake angle equal to – 5°. This fault plane solution is similar to the CMT mechanism, the main difference concerns the rake angle. In particular, the CMT solution shows a reverse component of roughly 50% of the strike component, while the latter solution shows an almost pure left-lateral strike slip solution on the NS plane (8% of normal component).

The computation of a fault plane solution using polarity data observed at local, regional, and teleseismic distances is complicated by the strong heterogeneities of the lithosphere present in Eastern Sicily, particularly to the North of the epicenter. Here, both the Etna volcano and the Tyrrhenian subduction may cause strong distortions of seismic rays traveling to regional distances ($\Delta \geq 2°$) in Northern Italy and Europe (Amato *et al.*, 1991b; Cocco *et al.*, 1991). We observe that regional stations between azimuth ~ 300° and ~ 40° have recorded compressions or dilatations not in agreement with the N-S vertical plane of the CMT strike-

slip solution. To account for these discrepancies, we hypothesize that rays from the hypocenter to the Northwest (*i.e.*, to stations in Northern Italy and France) are strongly bent, traveling around the Etna volcano (see fig. 1), and rays to the North pass through an extremely heterogeneous crust and upper mantle – *i.e.*, through the Tyrrhenian oceanic basin and the underlying subducting slab. In this latter case, the seismic rays may have take-off and azimuth angles different from those predicted for *Pn* phases. Moreover, theoretical take-off angles for *Pn* phases recorded north of the main shock epicenter are close to the EW trending nodal plane of the CMT solution. For these reasons, we have computed a fault plane solution by inverting polarity data with assigned weights: *Pn* have half of the weight assigned to the other phases. Figure 2b shows the focal mechanism resulting from such an inversion for which the polarities of regional data have smaller weights than those from local and teleseismic data. This fault plane solution is similar to the other two mechanisms previously discussed, but it shows a NS plane striking $190° \pm 15°$, dipping $80° \pm 25°$ to the west with a rake angle of $-10° \pm 20°$. All three solutions have almost vertical N-S planes (the dip angle of the NS plane ranges between 80° to the west and 84° to the east). The rake angle resulting from the polarity solution is similar to that of the moment tensor inversion solution.

Di Bona *et al.* (1994) discuss the *S*-wave polarization at the two closest strong motion recording sites, located to the northwest and to the southeast of the main shock epicenter, both at about 30 km distance. They found that the observed polarization does not agree with the *S*-wave polarization expected from the CMT fault plane solution. Because this feature may also be related to the local structure beneath the stations, we cannot stress more insight into focal mechanisms of the main shock.

The earthquake rupture cannot be easily related to a clear active fault, because (a) it is located offshore, Northwest of the Augusta peninsula (see fig. 1), where there are no mapped faults; and (b) it is relatively deep and too small ($M_L = 5.4$) to rupture throughout the upper crust up to the surface. Looking at the known tectonic structures (Bianchi *et al.*, 1987), we may infer that the earthquake occurred either on the ~ N-S trending Ibleo-Maltese scarp, or on a ~ E-W striking fault bordering the Iblean plateau, to the south, toward the Gela-Catania foredeep (fig. 1).

3. The temporary network of ING

A temporary seismic network was installed by ING within two days from the main shock of December 13. The network consisted of eight digital stations linked with digital telemetry to the mobile acquisition center, installed on a truck. Four stations were equipped with three-component sensors (two short-period Teledyne S-13, two broad-band Guralp CMG4-T), and four had only the vertical component (S-13). For the hypocentral locations and the computation of the focal mechanisms we have also used stations PZI, MEU, and GIO belonging to the ING National Network, as well as stations of local networks operating in the proximity (40-100 km) of the epicentral region.

Due to the initial uncertainity on the hypocenter location, and to the fact that the most extensive damage was reported in the towns of Lentini and Carlentini, 20-30 km onshore from the epicentral area, the temporary local network was installed in a broad region, with some stations (for instance TDA9, see fig. 3a-d) located as far as 40 km from the epicentral region. Once the first hypocentral locations were determined on the computer of the mobile acquisition center, station MDP9 was moved to the north (to site SGR9, see fig. 3a-d), to reduce the azimuthal gap of the network.

The seismic signals recorded at each site were digitized by a Lennartz 5800 system, with a dynamic range of 120 dB in gain-ranging mode (see Amato *et al.*, 1991a). The data were then transmitted with digital telemetry to the central system installed on the truck. One station (AUG9) has been recording locally on magnetic tape, because its location did not allow radio transmission to the acquisition center.

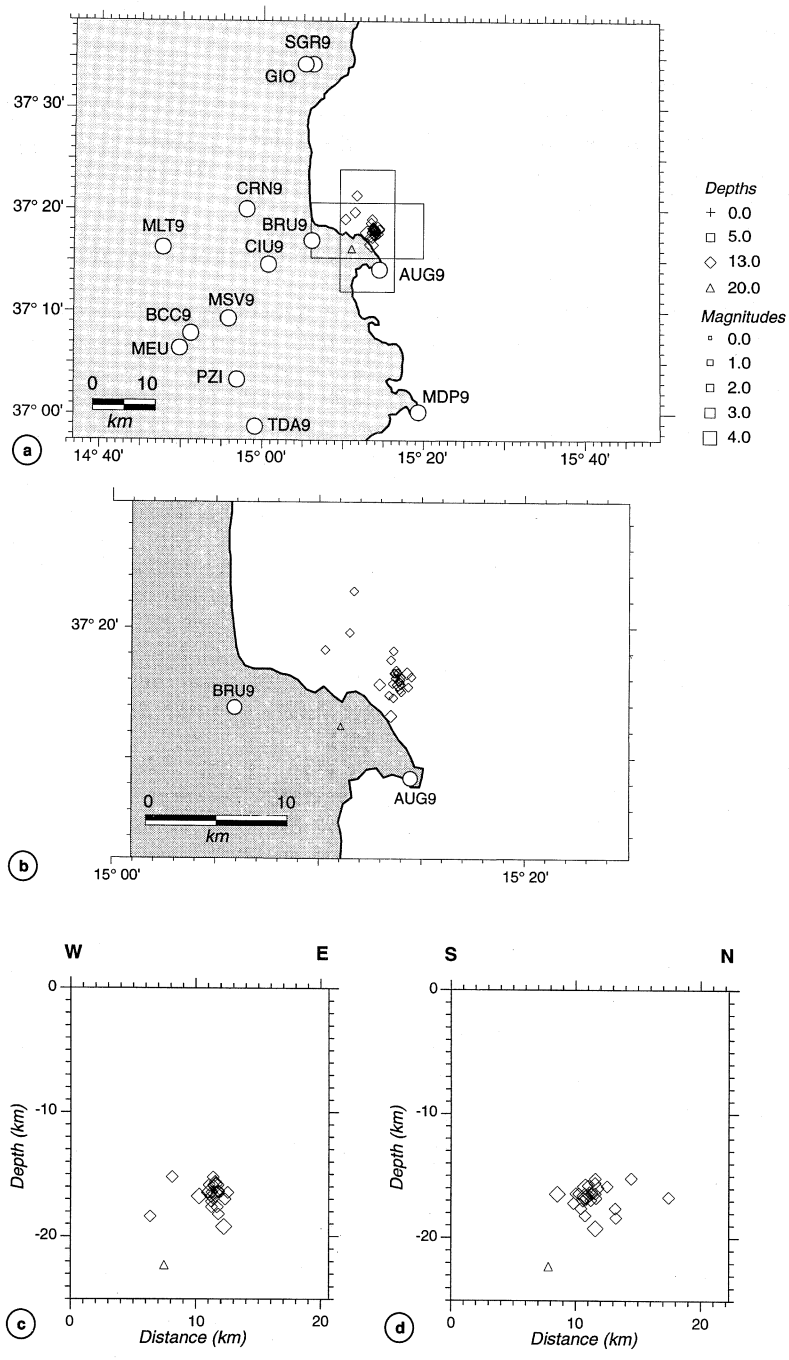

Fig. 3a-d. Seismic station geometry and aftershock distribution (a) and (b) closer map view. Two vertical cross sections are shown: c) W-E vertical section; d) S-N vertical section.

4. The aftershocks

The three days following the main shock (13-15 December) are characterized by a very low aftershock activity. In 30 min after the main event, only a few aftershocks were recorded, with a maximum magnitude of 2.7. The local network was fully operating by the morning of December 15. The overall network geometry is shown in fig. 3a. Up to December 16 (before 13:50 UTC) 7 more earthquakes with magnitudes between 2.1 and 2.7 (6 of them within the first 24 h) were recorded: the aftershock magnitudes and their number were unusually low for a magnitude 5.4 earthquake.

On December 16, at 13:50 UTC the seismic activity increased after the $M_L = 4.6$ event. This earthquake is the strongest aftershock, and it was recorded by both short-period and broad-band instruments of the mobile network. A sequence of aftershocks followed this earthquake (see fig. 4) with magnitudes (M_D) lower than 3.0. Most of the 300 earthquakes recorded by the local network were recorded only by the two closest stations, because of their small magnitudes ($M \leq 1.7$, that is the detection threshold of the network). Figure 4 shows the histogram of the number of events as a function of time. The paucity of aftershocks after the $M_L = 5.4$ main shock is evident; the seismic activity increased immediately after the $M_L = 4.6$ aftershock of December 16, and ceased after 19 days. This duration of the seismic sequence is anomalous for a magnitude 5.4 earthquake. The duration of the aftershock sequence predicted for a magnitude 5.4 event by the Gardner and Knopoff (1974) relation is about eight months (230 days). We cannot estimate the duration of aftershocks from previ-

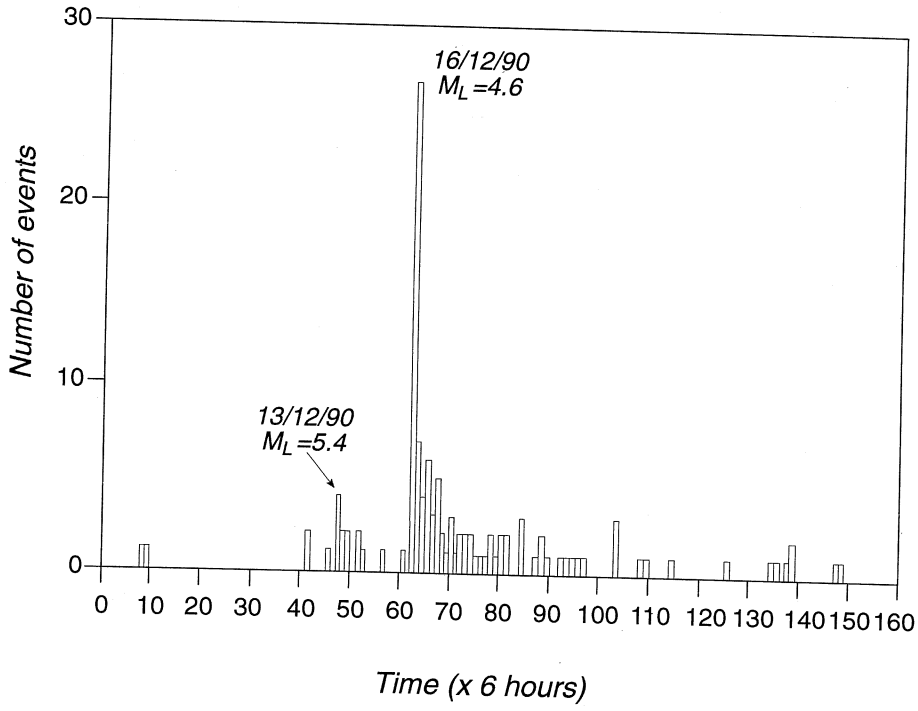

Fig. 4. Time distribution of earthquakes detected by the seismometric network in the study area. Time scale has to be multiplied for 6 h.

ously recorded seismic sequences because of the quiescence of the investigated region. The 1990 earthquake and its aftershocks provide the first instrumental recordings for this seismogenic area. The seismic activity finally ceased on January 5, 1991. Moreover, there is an anomalous absence of magnitude 4 earthquakes following the main shock (only 1 M_L 4.6 event after 3.5 days), with respect to the predictions of the frequency magnitude relationship.

The local magnitude M_L of the largest aftershock was computed by simulating the Wood-Anderson response from the digital recordings at the seismic stations of the mobile network. Figure 5a,b shows the synthetic Wood-Anderson simulated from the digital waveforms recorded at broad-band station MLT9, equipped with a Guralp CMG4-T strong motion seismometer. The M_L values estimated at this seismic station are 4.4 on the N-S (~ tangential) and 4.8 on the E-W (~ radial) component, respectively. The difference between the two horizontal components is due to a strong polarization of the *S* wave on the E-W component, as clearly visible in fig. 5a. Figure 5b shows the Fourier spectrum of the two components of ground velocity. This figure illustrates that the polarization effect occurs at low frequency, between 0.25 and 1.5 Hz, explaining why the M_L estimate from the Wood-Anderson seismogram (the W-A response is peaked at 1.25 Hz) on the EW component is higher. Moreover, we have to take into account that the local magnitude of the aftershock ($M_L = 4.6$) was computed from local data, while the local magnitude of the main shock

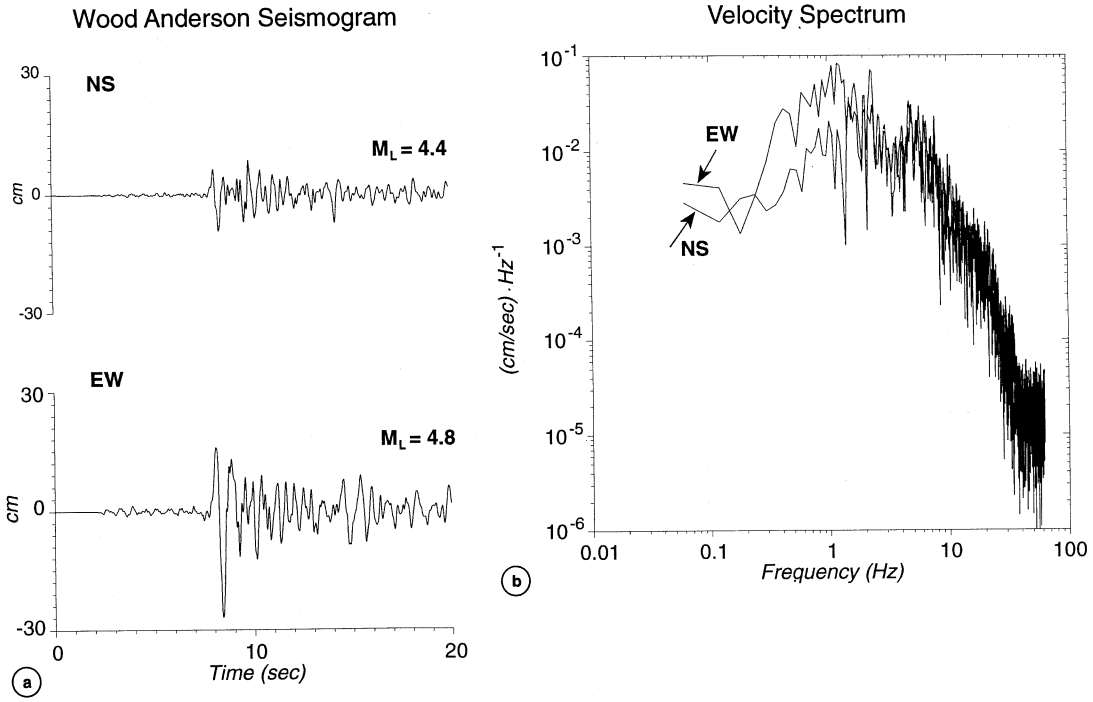

Fig. 5a,b. a) Horizontal components of the Wood-Anderson seismogram synthesized by the broad-band signal recorded at station MLT9, for the aftershock of December 16, 1990 (13:50 UTC); b) *S*-wave velocity spectrum of the horizontal components of the same earthquake.

($M_L = 5.4$) was computed from regional data. This suggests that the difference between the local magnitudes of these two earthquakes may be larger than that resulting from the estimated values.

We located about 50 aftershocks using arrival times at the seismic stations of the local network. As shown in fig. 4, only three days after the $M_L = 4.6$ event the activity was strongly reduced, with only two located earthquakes per day on the average. Due to poor knowledge of the Earth's structure in the region, we located the earthquakes after determining the best half-space velocity model. This was done looking at the *P*- and *S*-wave residuals, and at their standard deviation, for a suite of *P* velocity models (from 5.0 km/s to 7.0 km/s) and *Vp/Vs* ratios (from 1.5 to 2.0). As described in detail by Amato *et al.* (1991b), the best solution (*i.e.*, the one that minimizes the residuals) is for $Vp = 5.9$ km/s and $Vp/Vs = 1.75$-1.80. The *Vp/Vs* ratio was also calculated with a method independent from the hypocentral locations (see Soufleris *et al.*, 1982), that yields a value of 1.78, in agreement with the previous estimate. In order to evaluate the influence of the unfavorable network geometry on earthquake location, we ran a series of tests. We computed synthetic travel times with the actual source-receiver geometry, adding gaussian noise (with different standard deviations) to the theoretical travel times, and then recomputed the hypocenters using either only *P* data, or *P* and *S* data, and also varying the half-space velocity model (Amato *et al.*, 1991b). The results of these tests show that the network configuration computes reliable earthquake location with errors of about one kilometer, provided that we use *S* readings and the best halfspace velocity model. Since we have high-quality *S*-wave readings at least from four three-component stations, we are confident of the solutions obtained.

The activity following the $M_L = 4.6$ shock is clustered in a very narrow volume, of approximately $5 \times 2 \times 5$ km^3 (fig. 3a-d). The aftershocks seem to be slightly aligned in a N-S direction, although this elongation is within the location errors (± 1 km). The hypocentral depths range between 15 and 20 km. The cluster is located a few kilometers to the south of the main shock (fig. 4). The epicentral distance between the main shock of December 13, and the largest aftershock of December 16, is 4.8 km.

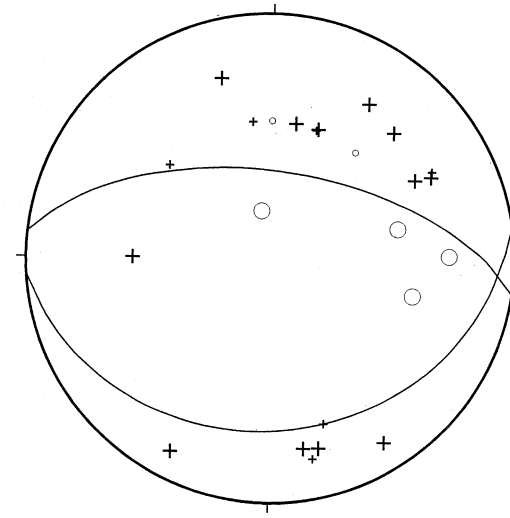

Fig. 6. Fault plane solution computed from polarity data for the $M_L = 4.6$ aftershock.

The fault plane solution computed for the largest aftershock shows a normal faulting mechanism, on EW trending planes (fig. 6). The north dipping plane has a strike angle of $276° \pm 10$, a dip of $60° \pm 10$ with a rake of $-84° \pm 10$. Although the solution is computed with a lower number of polarities compared to the main shock, the presence of many stations at small epicentral distances better constrains the solution. Figure 7 shows the three-components of ground velocity recorded at MLT9, and the behavior of horizontal polarization for *P*- and *S*-wave as a function of time. We note that there is almost a factor of 10 between *P*- and *S*-wave amplitudes, confirming that this station lies close to a nodal plane (in agreement with the focal mechanism reported in fig. 6). The analysis of *P*-wave polarization shows that the azimuth of the station is 276° (the azimuth resulting from the hypocentral determination is 269°), and that the incidence at the recording site is 30° (fig. 7). Finally, the

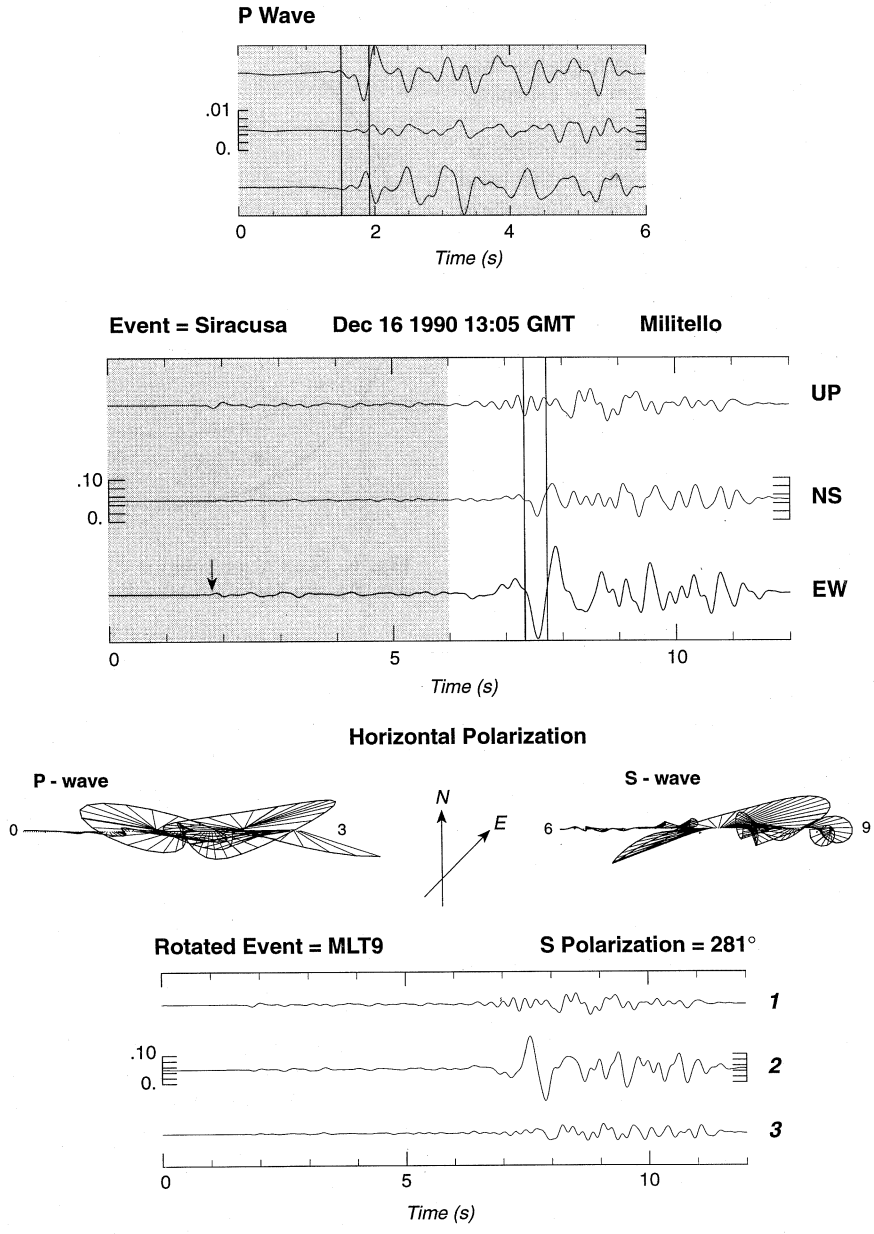

Fig. 7. *P*- and *S*-wave polarization at MLT9. The three components of ground velocity recorded during the $M_L = 4.6$ aftershock are shown. The shadowed area indicates the time window selected for the enlarged plot of *P*-waves (top of the figure). The arrow indicates the *P*-wave arrival time. There is a factor 10 between *P*- and *S*-wave amplitudes at this seismic station. The horizontal *P*- and *S*-wave polarizations are plotted; the amplitudes of the former have been multiplied by a factor of 10. The estimated *S*-wave polarization is 281°. The waveforms plotted at the bottom of the figure represent the recorded ground velocity rotated 281° from the north, indicating the direction of maximum *S*-wave polarization.

S-wave polarization observed at MLT9 is 281°, that is close to the theoretical *S*-wave polarization (295°) computed from the focal mechanism shown in fig. 6 using a takeoff angle of 116° (resulting from the hypocentral location, while azimuth and incidence angle have been computed from *P*-wave polarization). The analysis of *S*-wave polarization at MLT9 strongly constrains the fault plane solution shown in fig. 6. The similarity of the waveforms recorded for the $M_L = 4.6$ event and for its aftershocks, suggests a similar mechanism for the earthquakes of this sequence. This is also confirmed by the composite solution computed for these earthquakes by Cocco *et al.* (1991).

By using the broad-band recordings we computed the seismic moment and the corner frequency of the $M_L = 4.6$ aftershock, that are 2.1×10^{23} dyne·cm, and 2.4 Hz, respectively. The moment magnitude (Hanks and Kanamori, 1979) for this aftershock is 4.9. By assuming an omega square spectral model with constant stress drop, these values yield a Brune stress drop of 75 bar. Di Bona *et al.* (1994) computed a stress drop larger than 500 bar for the main shock, much larger than that obtained for the $M_L = 4.6$ aftershock.

5. Concluding remarks

The December 13, 1990 $M_L = 5.4$ Eastern Sicily earthquake occurred offshore Augusta at 37.34N and 15.26E. The hypocentral depth resulting from the master-event location yields a reasonable estimate of 22 ± 2 km, slightly below the depth of the aftershocks. The CMT fault plane solution, the focal mechanism obtained from moment tensor inversion at regional distance (Giardini *et al.*, 1994), and the polarity solution, show a similar strike slip mechanism for this event, with either left-lateral motion on a NS vertical plane, or right-lateral motion on an EW plane. The solution indicates a SE-NW direction of compression, associated with NE-SW extension, that is in agreement with the regional tectonic stress.

The mainshock was been followed by an unusual quiescence. The three days following the mainshock (13-15 December) are characterized by very low activity without the *M*4 and *M*3 shocks expected after an $M_L = 5.4$. On December 16, the largest aftershock ($M_L = 4.6$) occurred, with a fault plane solution showing normal faulting on EW trending planes, different from the mainshock strike-slip mechanism. The fault plane solution of the largest aftershock is consistent with the observed *S*-wave polarization. Thanks to the local network installed after the mainshock, we were able to locate 50 aftershocks which occurred after December 16. The distribution of the aftershocks delineates an area of approximately $5 \times 2 \times 5$ km^3, slightly elongated in a NS direction between 15 and 20 km depth. The mainshock epicenter is at 4.8 km and N14°E from the epicenter of the largest aftershock, and is located at the base of the seismogenic zone of the aftershock cluster.

The quiescence that followed the mainshock, the paucity of large aftershocks, and the different focal mechanism between the mainshock (strike slip) and the $M_L = 4.6$ event (normal) suggest that the $M_L = 5.4$ earthquake is an isolated shock and that the aftershock activity is linked to the $M_L = 4.6$ event rather than to the mainshock. This conclusion is also supported by the lower stress drop of the largest aftershock (75 bar) with respect to the stress drop estimated for the main shock by Di Bona *et al.* (1994) ($\Delta\sigma \geq 500$ bar). A seismic sequence with one $M_L = 5.4$ earthquake, one $M_L = 4.6$ event and numerous aftershocks with magnitude less or equal to 3.0 does not agree with the frequency-magnitude relationship. In this sense we define the main shock as an isolated event, considering also the temporal gap between the two strongest events (more than three days). The Gutenberg-Richter frequency-magnitude relationship is satisfied by the $M_L = 4.6$ events and the other aftershocks with a b value close to 1.

In conclusion, the December 13, 1990 earthquake occurred in a seismogenic area that experienced large earthquakes in the past, where the expected maximum magnitude for a characteristic earthquake is of the order of 7 ($M_0 \approx 10^{27}$ dyne·cm). The seismic moment of the 1990 Syracuse earthquake is 3.7×10^{17} Nm,

thus representing a small fraction of the expected energy release. These considerations suggest that the 1990 earthquake did not reduce the seismogenic potential in Eastern Sicily.

Acknowledgements

We wish to thank the researchers and the technicians of the Istituto Nazionale di Geofisica who helped us to deploy the local network and to maintain the instruments. Daniela Riposati deserves particular thanks for drawing the figures.

REFERENCES

AMATO, A., R. AZZARA, A. BASILI, L. BERANZOLI, C. CHIARABBA, M. COCCO, M. DI BONA, S. MAZZA, F. MELE and G. SELVAGGI (1991a): L'intervento della Rete Sismica Mobile in occasione del terremoto del 13 dicembre nella Sicilia orientale, *Publication of the Istituto Nazionale di Geofisica*, Roma, n. 537, 45-56 (in italian).

AMATO, A., R. AZZARA, A. BASILI, C. CHIARABBA, M. COCCO, M. DI BONA and G. SELVAGGI (1991b): La sequenza sismica del dicembre 1990 nella Sicilia orientale: analisi dei dati sismometrici, *Publication of the Istituto Nazionale di Geofisica*, Roma, n. 537, 57-83 (in italian).

BARBANO, M.S. and M. COSENTINO (1981): Il terremoto Siciliano dell'11 Gennaio 1693, *Rend. Soc. Geol. Ital.*, **4**, 517-522.

BASILI, A., R. CONSOLE and F. MELE (1990): Automatic procedures for seismic event location, in *Proceedings of the ECE/UN Seminar on Prediction of Earthquakes*, edited by CARLOS S. OLIVEIRA, vol. 1, Lisbon.

BOSCHI, E., E. GUIDOBONI and D. MARIOTTI (1994): Seismic effects of the strongest hystorical earthquakes of the Siracusa area, *Annali di Geofisica*, **38**, 223-253 (this volume).

BIANCHI, F., S. CARBONE, M. GRASSO, G. INVERNIZZI, F. LENTINI, G. LONGARETTI, S. MERLINI and F. MOSTARDINI (1987): Sicilia orientale: profilo gelogico Nebrodi-Iblei, *Mem. Soc. Geol. Ital.*, **38**, 429-458.

CARBONE, S., M. GRASSO and F. LENTINI (1982): Considerazioni sull'evoluzione geodinamica della Sicilia sud-orientale dal Cretaceo al Quaternario, *Mem. Soc. Geol. Ital.*, **24**, 367-386.

COCCO, M., A. AMATO, R. AZZARA, A. BASILI, E. BOSCHI, C. CHIARABBA, M. DI BONA, D. GIARDINI, N.A. PINO, A. ROVELLI and G. SELVAGGI (1991): The December 13, 1990 Eastern Sicily earthquake (M_L 5.4), *EOS*, AGU Fall Meeting, **72**, p. 311.

DI BONA, M., M. COCCO, A. ROVELLI, R. BERARDI and E. BOSCHI (1994): Analysis of strong motion data of the 1990 Eastern Sicily earthquake, *Annali di Geofisica*, **38**, 283-300 (this volume).

GARDNER, J.K. and L. KNOPOFF (1974): Is the sequence of earthquakes in Southern California, with aftershocks removed, poissonian? *Bull. Seismol. Soc. Am.*, **64**, 1363-1367.

GIARDINI, D., B. PALOMBO and N.A. PINO (1994): Long-period modelling of MEDNET waveforms for the December 13, 1990 Eastern Sicily earthquake, *Annali di Geofisica*, **38**, 267-282 (this volume).

HANKS, T.C. and H. KANAMORI (1979): A moment magnitude scale, *J. Geophys. Res.*, **84**, 2348-2350.

P.F.G. - Progetto Finalizzato Geodinamica (1985): Atlas of isoseismal maps of Italian earthquakes, edited by D. POSTPISCHL, *Quaderni della Ricerca Scientifica*, **114**, 2A.

SOUFLERIS, C., J.A. JACKSON, G.C.P. KING, C.P. SPENCER and C.H. SCHOLZ (1982): The 1978 earthquake sequence near Thessaloniki (Northern Greece), *Geophys. J. R. Astron. Soc.*, **68**, 429-458.